A multimode analysis of the gas-phase photoelectron spectra in oligoacenes

M. Malagoli, V. Coropceanu, D. A. da Silva Filho, and J. L. Brédas

Citation: J. Chem. Phys. **120**, 7490 (2004); doi: 10.1063/1.1687675
View online: http://dx.doi.org/10.1063/1.1687675
View Table of Contents: http://jcp.aip.org/resource/1/JCPSA6/v120/i16
Published by the American Institute of Physics.

A multimode analysis of the gas-phase photoelectron spectra in oligoacenes

M. Malagoli
Parallel Quantum Solutions, Fayetteville, Arkansas 72703-2600

V. Coropceanu, D. A. da Silva Filho, and J. L. Brédas
School of Chemistry and Biochemistry, Georgia Institute of Technology, Atlanta, Georgia 30332-0400

(Received 18 August 2003; accepted 29 January 2004)

We present a multimode vibrational analysis of the gas-phase ultraviolet photoelectron spectra of the first ionization in anthracene, tetracene, and pentacene, using electron-vibration constants computed at the density functional theory level. The first ionization of each molecule exhibits a high-frequency vibronic structure; it is shown that this regularly spaced feature is actually the consequence of the collective action of several vibrational modes rather than the result of the interaction with a single mode. We interpret this feature in terms of the missing mode effect. We also discuss the vibronic coupling constants and relaxation energies obtained from the fit of the photoelectron spectra with the linear vibronic model. © *2004 American Institute of Physics.* [DOI: 10.1063/1.1687675]

I. INTRODUCTION

In π-conjugated systems, the strong coupling between the geometric structure and the electronic structure controls the transport properties.[1–3] At the microscopic level, the hopping charge transport mechanism can often be described as a self-exchange electron transfer (ET) process from a charged, relaxed molecule to an adjacent neutral molecule. In the context of semiclassical ET theory and extensions thereof,[4–7] there are two major parameters that determine the self-exchange ET rate and ultimately the charge mobility: (i) the electronic coupling H_{ab} (transfer integral) between adjacent molecules/segments; and (ii) the reorganization energy λ. For efficient transport, H_{ab} needs to be maximized and λ minimized.

The reorganization energy is usually expressed as the sum of inner and outer contributions. The inner (intramolecular) reorganization energy arises from the change in equilibrium geometry of the donor and acceptor sites consecutive to the gain or loss of electronic charge upon ET. The outer reorganization energy is due to the polarization/relaxation of the surrounding medium. Due to the weakness of the van der Waals interactions among organic molecules, the separation of the reorganization energy into inter- and intramolecular contributions remains largely valid even in the case of molecular crystals.[8,9]

The reorganization energy is a measure of the strength of the interaction between the electronic structure and the vibrational states of the molecule and of the material[10–12] (a detailed knowledge of the electron–phonon coupling is thus needed for the complete understanding of the charge transport properties). The characterization of the contributions of each vibrational mode to λ is important to rationalize the temperature dependence of the electron-transfer rates.[12]

Here, we focus on the intramolecular reorganization energy and its vibrational mode description. We have recently exploited gas-phase ultraviolet photoelectron spectroscopy (UPS) data to estimate the intramolecular reorganization energy of anthracene, tetracene, and pentacene (see the chemical structures in Fig. 1).[13,14] The vibrational structure of the first ionization peaks was deconvoluted and analyzed in the framework of a two-mode harmonic model to obtain an estimate of λ. Although the estimated values were in good general agreement with the results of the theoretical calculations, there remained a notable disagreement on the role of low-frequency modes. Here, we present a multimode vibrational analysis of the UPS data using the vibrational frequencies and electron-vibration constants computed at the density functional theory (DFT) level. We show that the regular vibrational structure of the first ionization is a consequence of the collective action of several vibrational modes rather than of the interaction with a particular mode. We emphasize that the oligoacenes are of practical interest due to their large intrinsic mobilities[8,9,15] and have been used in the field of organic semiconductors as test systems for charge-transport theories.[16,17]

II. METHODOLOGY

A. Reorganization energy

Figure 2 represents the potential energy surfaces for electronic states 1 and 2 corresponding in the context of this work to the neutral state and the cation state of the molecule. The intramolecular reorganization energy for self-exchange consists of two terms related to the geometry relaxation energies upon going from the neutral-state geometry to the charged-state geometry and vice versa,[7–9,18,19]

$$\lambda = \lambda_{\mathrm{rel}}^{(1)} + \lambda_{\mathrm{rel}}^{(2)}, \tag{1}$$

$$\lambda_{\mathrm{rel}}^{(1)} = E^{(1)}(\mathrm{M}^{+\bullet}) - E^{(0)}(\mathrm{M}^{+\bullet}), \tag{2}$$

$$\lambda_{\mathrm{rel}}^{(2)} = E^{(1)}(\mathrm{M}) - E^{(0)}(\mathrm{M}). \tag{3}$$

Here, $E^{(0)}(\mathrm{M})$ and $E^{(0)}(\mathrm{M}^{+\bullet})$ are the ground-state energies of the neutral and cation states, respectively; $E^{(1)}(\mathrm{M})$ is the

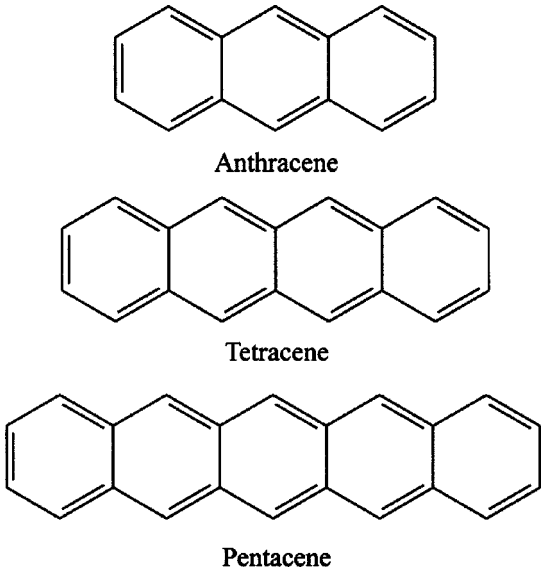

FIG. 1. Molecular structures of anthracene, tetracene, and pentacene.

energy of the neutral molecule at the optimal cation geometry and $E^{(1)}(M^{+\bullet})$ is the energy of the cation state at the optimal geometry of the neutral molecule.

The contribution of each vibrational mode to λ_{rel} can be obtained by expanding the potential energies of the neutral and cation states in a power series of the normal coordinates (denoted here as $\mathbf{Q}_1$ and $\mathbf{Q}_2$). In the harmonic approximation, the relaxation energy λ_{rel} writes[7,19]

$$\lambda_{rel}=\sum \lambda_i=\sum \hbar\omega_i S_i, \tag{4}$$

$$\lambda_i=\frac{k_i}{2}\Delta Q_i^2, \quad S_i=\lambda_i/\hbar\omega_i. \tag{5}$$

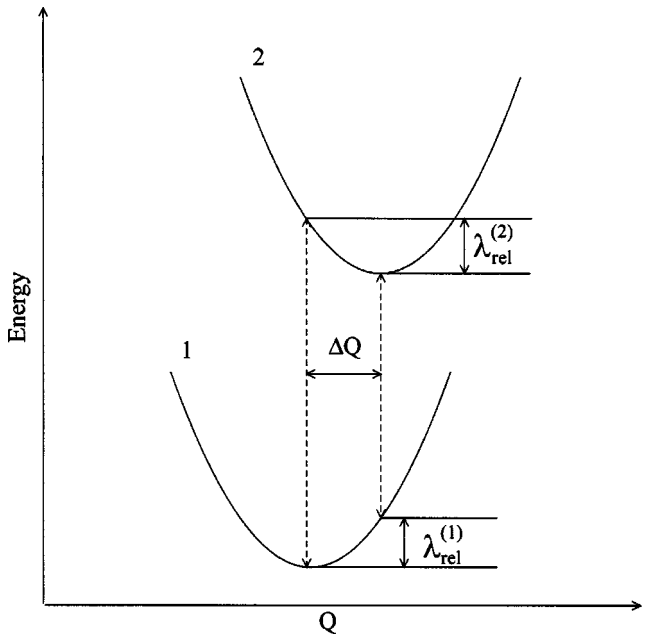

FIG. 2. Sketch of the potential energy surfaces for neutral state 1 and cation state 2, showing the vertical transitions (dashed lines), the normal mode displacement ΔQ, and the relaxation energies $\lambda_{rel}^{(1)}$ and $\lambda_{rel}^{(2)}$.

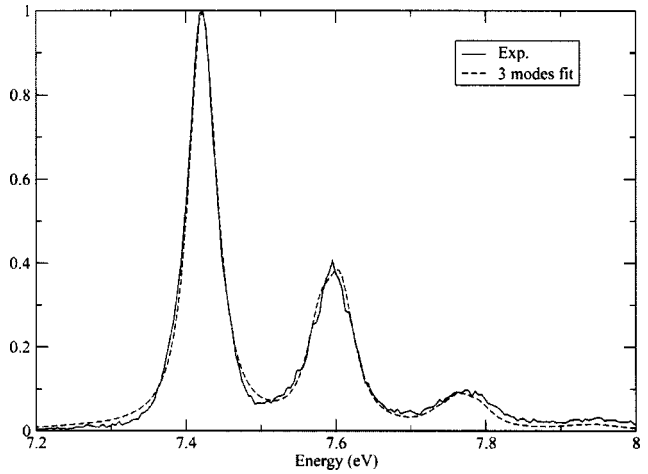

FIG. 3. Three-mode fit of the vibrational structure of the first UPS ionization peak of anthracene. The parameters used in the fit are reported in Table II.

Here, the summations run over the vibrational modes; ΔQ_i represents the displacement along normal mode i between the equilibrium positions of the two electronic states of interest; k_i and ω_i are the corresponding force constants and vibrational frequencies. For the sake of further discussion, we have included in Eq. (4) the representation of the reorga-

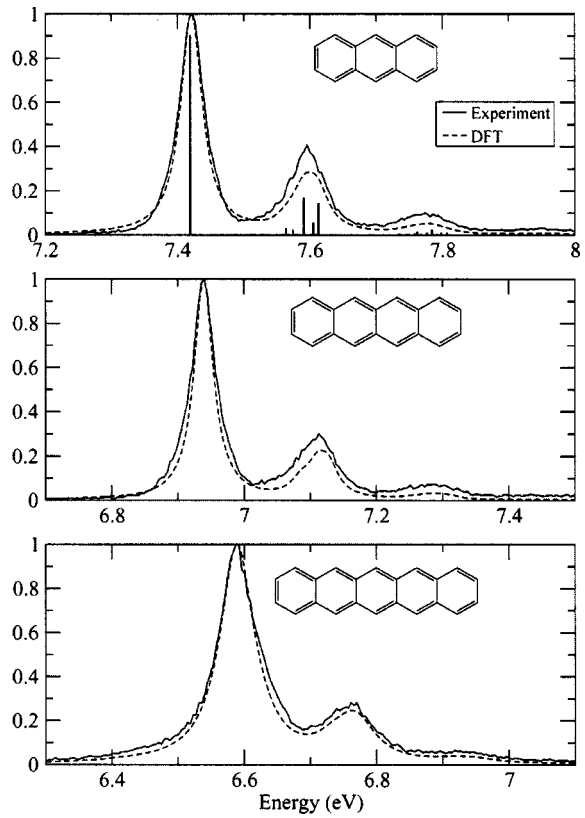

FIG. 4. DFT/B3LYP simulation of the vibrational structure of the UPS first ionization peak of anthracene, tetracene, and pentacene. The normal modes of the cation species with the largest Huang–Rhys factors (see Tables III–V) have been used for the simulations. A scaling factor of 0.9613 has been applied to the computed frequencies. The transition intensities were convoluted with Lorentzian functions with FWHM of 0.046, 0.046, and 0.060 eV for anthracene, tetracene, and pentacene, respectively.

TABLE I. Vibrational energies, ω (cm^{-1}), Huang–Rhys factors, S, and relaxation energies, λ_{rel} (meV), obtained from the analysis of the UPS spectra (Refs. 13, 14) of anthracene, tetracene, and pentacene.

	Anthracene			Tetracene			Pentacene		
	ω (cm^{-1})	S	λ_{rel} (meV)	ω (cm^{-1})	S	λ_{rel} (meV)	ω (cm^{-1})	S	λ_{rel} (meV)
Mode 1	341	0.182	7.7	330	0.184	7.6	483	0.279	16.7
Mode 2	1398	0.358	62.0	1404	0.294	51.2	1348	0.251	41.9
Total			69.7			58.8			58.6

nization energy in terms of the Huang–Rhys factors S_i. We note that the Huang–Rhys factors are directly related to the Δ_i terms, which are largely used in the literature and are the dimensionless counterparts of the projections $\Delta Q_i : S_i = \Delta_i^2/2$.

The numerical procedure consists of the following steps: First, the normal-mode coordinates and the force constants are determined. The standard rectangular normal modes $\mathbf{Q}_{1(2)}$ are obtained as a linear combination of Cartesian displacements,[20]

$$Q_{1(2)i} = \sum_j L_{1(2)ji}(q_{1(2)j} - q^{(0)}_{1(2)j}). \tag{6}$$

Here, the matrix $\mathbf{L}_{1(2)}$ connects the $3n$-6 [n is the number of atoms in the (nonlinear) molecule] normal coordinates with the set of $3n$ mass-weighted Cartesian coordinates $\mathbf{q}_{1(2)}$; the vectors $\mathbf{q}_1^{(0)}$ and $\mathbf{q}_2^{(0)}$ correspond to the stationary points on the adiabatic potential surfaces of states 1 and 2, respectively. Then, the normal mode displacements $\Delta\mathbf{Q}_{1(2)}$ are obtained by projecting the displacements $\Delta\mathbf{q} = \mathbf{q}_1^{(0)} - \mathbf{q}_2^{(0)}$ onto the normal-mode vectors. Finally, substituting the calculated quantities into Eqs. (5) and (4), the Huang–Rhys factors and the total relaxation energy are obtained.

It is important to note that the normal modes of the neutral and cation states, $\mathbf{Q}_1$ and $\mathbf{Q}_2$, are in general different and are related by a transformation consisting of a multidimensional rotation and a translation,[21]

$$Q_1 = JQ_2 + \Delta Q. \tag{7}$$

J is the Duschinsky matrix describing the mixing of the normal coordinates of the two states.

We performed geometry optimizations for the neutral and radical-cation states of anthracene, tetracene, and pentacene, followed by calculation of harmonic vibrational frequencies and normal modes. The calculations were achieved at the DFT level using the B3LYP functional, involving the exchange functional by Becke,[22,23] and the correlation functional by Lee, Yang, and Parr.[24] The basis set used is the split-valence plus polarization 6-31G**;[25–29] all the calculations were performed with the GAUSSIAN 98 program.[30]

B. Franck–Condon analysis of the UPS spectra

In the framework of the Born–Oppenheimer (adiabatic) and Franck–Condon (FC) approximations, the shape of an ionization band is governed by the overlap (Franck–Condon) integrals $\mathrm{FCI}(m,n) = \langle \Phi_m(Q_1) | \Phi_n(Q_2) \rangle$ of the vibrational functions [$\Phi_m(Q_1)$ and $\Phi_n(Q_2)$] of the neutral and cation ground electronic states. Several methods have been proposed to calculate multidimensional Franck–Condon (FC) integrals.[31–35] The calculations are considerably simplified when Duschinsky mixing is neglected, i.e., $\mathbf{J}=1$ in Eq. (7). In this case, referred to as the parallel mode approximation,[31] the relative intensity of a multidimensional vibrational transition, involving p vibrational modes, is obtained as a simple product of one-dimensional FC integrals,[36]

$$I(m_1,n_1,m_2,n_2,\ldots,m_p,n_p) = \prod_{i=1}^{p} \mathrm{FCI}(m_i,n_i)^2 \exp\left\{\frac{-\hbar m_i \omega_i}{k_B T}\right\}, \tag{8}$$

$$\mathrm{FCI}(m,n)^2 = \exp\{-S\} S^{(n-m)} \frac{m!}{n!} [L_m^{(n-m)}(S)]^2, \tag{9}$$

where m_i and n_i are the initial and final vibrational quantum numbers of the mode ω_i, k_B is the Boltzmann constant, T is

TABLE II. Wave numbers ω (cm^{-1}), Huang–Rhys coefficients, S, and relaxation energies, λ_{rel} (eV), obtained by a linear vibronic model fitting of the shape of the first ionization peak for anthracene, tetracene, and pentacene.[a]

	Anthracene			Tetracene			Pentacene		
	ω (cm^{-1})	S	λ_{rel} (meV)	ω (cm^{-1})	S	λ_{rel} (meV)	ω (cm^{-1})	S	λ_{rel} (eV)
Mode 1	109	0.122	2	158	0.080	2	346	0.088	4
Mode 2	1272	0.210	33	1179	0.147	22	1207	0.100	15
Mode 3	1493	0.277	51	1457	0.251	45	1454	0.176	32
Total			87			69			51

[a]Three vibrational modes have been included in the least square fitting procedure. The transition intensities were convoluted with Lorentzian functions with full width at half maximum of 0.046, 0.046, and 0.060 eV for anthracene, tetracene, and pentacene, respectively.

TABLE III. DFT/B3LYP estimates of frequency, ω (cm^{-1}), Huang–Rhys factors, S, and relaxation energies, λ_{rel} (meV), for the totally symmetric vibrations of anthracene in its neutral and cation states.

Neutral			Cation		
ω (cm^{-1})	S	λ_{rel} (meV)	ω (cm^{-1})	S	λ_{rel} (meV)
399	0.001	0	396	0.001	0
641	0.000	0	626	0.000	0
766	0.003	0	766	0.002	0
1038	0.002	0	1057	0.000	0
1194	0.021	3	1207	0.026	4
1301	0.048	8	1291	0.019	3
1443	0.094	17	1426	0.150	27
1530	0.010	2	1545	0.048	9
1607	0.194	39	1611	0.127	25
3171	0.000	0	3195	0.000	0
3180	0.000	0	3206	0.000	0
3205	0.001	0	3228	0.000	0
Total		69			68
Total (AP)[a]		69			68

[a]Values computed from the adiabatic potential energy surfaces.

the temperature, and $L_n^{\alpha}(x)$ is a Laguerre polynomial. Note that the square of the Franck–Condon integral is referred to as the Franck–Condon factor (FCF). If only transitions from the vibrational ground state ($m=0$) are considered, the temperature-averaged FCFs [Eq. (8)] turn into the standard Poisson distribution,

$$I(m=0,n)=\frac{S^n}{n!}e^{-S}. \tag{10}$$

III. RESULTS AND DISCUSSION

The gas-phase photoelectron spectra of anthracene, tetracene, and pentacene obtained in our previous work[13,14] are shown in Figs. 3 and 4. For each molecule, several ionizations, including the first ionization, contain partially resolved vibrational fine structure. The experimental spectra have been deconvoluted using a series of Gaussian to allow a quantitative analysis of the vibrational structures. The first ionization of each molecule clearly exhibits a high frequency progression of about 1400 cm^{-1}. The intensity of this progression resembles a Poisson distribution. There is, however, additional contribution from one or more vibrations. The results of spectral fits with one additional low-frequency mode are given in Table I. For all three molecules, the largest contribution to λ_{rel} is from the higher energy vibrational frequency. The contribution of the low-frequency mode is equal for anthracene and tetracene and accounts for about 11%–13% of the total intensity; in pentacene, this contribution rises up to 30%. Note, however, that the progression associated with the low-frequency mode is not described by the harmonic model as well as the high frequency progression.[13,14]

A. Fitting of the experimental photoelectron spectra

In order to check for possible shortcomings of the deconvolution procedure used in the former analysis, we have fitted the experimental spectrum using vibrational progressions that strictly satisfy the linear vibronic model [Eqs. (8) and (9)]. In the fitting procedure, the values of vibrational frequencies and Huang–Rhys factors associated with a vibrational mode are optimized in order to minimize the sum of the squares of the deviations between experimental and com-

TABLE IV. DFT/B3LYP estimates of frequency, ω (cm^{-1}), Huang–Rhys factors, S, and relaxation energies, λ_{rel} (eV), for the totally symmetric vibrations of tetracene in its neutral and cation states.

Neutral			Cation		
ω (cm^{-1})	S	λ_{rel} (meV)	ω (cm^{-1})	S	λ_{rel} (meV)
318	0.007	0	317	0.007	0
634	0.000	0	629	0.000	0
766	0.002	0	766	0.001	0
872	0.001	0	880	0.001	0
1030	0.005	1	1051	0.001	0
1190	0.014	2	1202	0.021	3
1235	0.045	7	1247	0.043	7
1426	0.053	9	1421	0.020	4
1438	0.037	7	1440	0.099	18
1492	0.008	1	1491	0.000	0
1570	0.029	6	1557	0.050	10
1591	0.120	24	1597	0.079	16
3175	0.000	0	3196	0.000	0
3180	0.000	0	3205	0.000	0
3205	0.001	0	3226	0.000	0
Total		57			57
Total (AP)[a]		57			56

[a]Values computed from the adiabatic potential energy surfaces.

TABLE V. DFT/B3LYP estimates of frequency, ω (cm^{-1}), Huang–Rhys factors, S, and relaxation energies, λ_{rel} (eV), for the totally symmetric vibrations of pentacene in its neutral and cation states.[a]

Neutral			Cation		
ω (cm^{-1})	S	λ_{rel} (meV)	ω (cm^{-1})	S	λ_{rel} (meV)
264	0.031	1	263	0.030	1
616	0.000	0	613	0.000	0
646	0.000	0	636	0.000	0
765	0.001	0	765	0.000	0
800	0.003	0	807	0.002	0
1027	0.006	1	1046	0.004	1
1190	0.009	1	1200	0.015	2
1218	0.044	7	1227	0.043	7
1345	0.001	0	1338	0.004	1
1425	0.074	13	1425	0.003	1
1448	0.013	2	1441	0.097	17
1506	0.002	0	1515	0.000	0
1569	0.093	18	1560	0.059	11
1590	0.011	2	1590	0.033	7
3166	0.000	0	3192	0.000	0
3171	0.000	0	3196	0.000	0
3175	0.001	0	3202	0.000	0
3201	0.001	0	3224	0.001	0
Total		47			48
Total (AP)[a]		49			48

[a]Values computed from the adiabatic potential energy surfaces.

TABLE VI. Portion of the A_g block of the Duschinsky matrix for anthracene.

		Cation								
	ω/cm^{-1}	1057	1207	1291	1426	1545	1611	3195	3206	3228
	1038	−0.988	−0.102	0.038	−0.095	−0.013	0.054			
	1194	0.094	−0.991	−0.076	0.052	−0.015	−0.009			
	1301	−0.014	0.057	−0.955	−0.289	−0.027	−0.007			
	1443	−0.100	0.061	−0.279	0.944	−0.048	0.124			
Neutral	1530	−0.034	−0.008	−0.046	0.067	0.962	−0.259			
	1607	−0.060	0.013	−0.014	0.100	−0.268	−0.956			
	3171							−0.984	0.179	−0.006
	3180							0.178	0.978	−0.110
	3205							0.014	0.109	0.994

puted spectra (using a conventional Levenberg–Marquardt algorithm). Lorentzian functions are used to convolute the transition intensities. We have performed several fits where we increased the number of vibrational modes involved and found that at least three modes were necessary to accurately reproduce the spectral shapes; adding more than three modes did not significantly improve the fit. The results of the fits are reported in Table II. To illustrate the quality of the procedure, the fitted spectrum obtained in the case of anthracene is reported in Fig. 3. We obtained similar results for tetracene and pentacene.

The results of a multimode analysis are in general agreement with the previous findings,[13] indicating that the main contribution to λ_{rel} comes from high-energy vibrations. These contributions account for 97%, 97%, and 92% of the relaxation energy for anthracene, tetracene, and pentacene, respectively; such contributions are about 10%–20% larger than previously estimated. The fits also indicate a small contribution from low energy modes, around 100–350 cm^{-1}, accounting for about 3%–8% of the total relaxation energy. Thus, the low-energy vibrational contributions to λ_{rel} obtained in the present work is about one-fourth the value that was estimated from the deconvolution procedure. The present results indicate that while the total relaxation energy derived in our previous study[13,14] was accurate, the contribution of low-frequency modes was overestimated.

B. Simulation of the UPS spectra using quantum-mechanical results

The results of the DFT/B3LYP calculations of relaxation energy for anthracene, tetracene, and pentacene are reported in Tables III–V, where λ_{rel} is partitioned into contributions from the vibrational modes. The total relaxation energies obtained from the normal mode analysis are in excellent agreement with the values computed directly from the adiabatic potential energy surfaces. The derived values are also in good agreement with previous calculations.[11,37] The theoretical calculations confirm that the main contribution to the relaxation energy comes from high-energy vibrations. This high-energy contribution is in fact divided over several vibrational modes with wave numbers in the range 1200–1600 cm^{-1}. The contribution to λ_{rel} from low-energy vibrations is negligible in anthracene and tetracene, and very small in the case of pentacene; this fully supports the concussion drawn from the results described in the previous section.

As a further check of the reliability of the DFT/B3LYP estimates, we have carried out the Franck–Condon simulation of the shape of the first ionization peak using the frequencies and Huang–Rhys factors from Tables III–V. The calculations were performed for the temperatures of 372, 452, and 507 K at which the UPS data were collected for anthracene, tetracene and pentacene, respectively. The position of the 0–0 transitions has been chosen to match the maximum of the experimental first ionization peak, corresponding to 7.421, 6.939, and 6.589 eV for anthracene, tetracene, and pentacene, respectively. A scaling factor $f = 0.9613$ has been applied to the computed vibrational frequencies, following the recommendations given for the comparison of B3LYP and experimental IR frequencies.[38]

The results of the simulation are shown in Fig. 4. In general, the positions and shapes of the peaks are very well reproduced. For anthracene and tetracene, the intensity of the second peak is slightly underestimated. Nevertheless, taking into account that the parameters have not been adjusted, the

TABLE VII. Portion of the A_g block of the Duschinsky matrix for tetracene.

		Cation							
	ω/cm^{-1}	1247	1421	1440	1491	1557	1597	3196	3205
	1235	−0.992	−0.113	−0.016	−0.025	−0.009	−0.016		
	1426	−0.045	0.299	0.941	−0.082	−0.127	−0.009		
	1438	−0.085	0.846	−0.318	−0.384	−0.102	0.112		
Neutral	1492	0.057	−0.298	0.064	−0.870	0.327	−0.196		
	1570	−0.045	0.261	0.062	0.274	0.918	−0.077		
	1591	0.001	−0.133	0.061	−0.110	0.150	0.970		
	3175							−0.961	0.275
	3180							0.275	0.958

TABLE VIII. Portion of the A_g block of the Duschinsky matrix for pentacene.

		Cation								
	ω/cm^{-1}	1338	1425	1441	1515	1560	1590	3192	3196	3202
	1345	−0.967	0.196	−0.158	0.015	0.004	0.007			
	1425	−0.197	−0.222	0.945	0.117	−0.069	0.017			
	1448	−0.154	−0.920	−0.237	−0.149	−0.142	−0.162			
	1506	−0.022	0.061	0.137	−0.953	0.181	0.188			
Neutral	1569	0.022	0.088	−0.036	−0.092	−0.905	0.403			
	1590	−0.023	−0.220	−0.073	0.216	0.351	0.880			
	3166							−0.992	−0.107	0.060
	3171							0.121	−0.940	0.318
	3175							−0.023	−0.323	−0.945

overall agreement between simulated and experimental spectra is excellent.

These results underline the importance of multimode effects to obtain a detailed understanding of the UPS band shapes in oligoacenes. The present simulations indeed indicate that the contribution ascribed in our previous study[13,14] to a low-frequency mode is more likely a result of multimode effects. In addition, the regular high-frequency vibrational progression is also the result of the action of several modes: As seen from the stick spectrum of anthracene in Fig. 4, five modes with energies of 1611, 1545, 1426, 1291, and 1207 cm^{-1} are involved in this case. However, the individual vibrational lines due to the damping are not fully resolved [we also note that the spacing between the vibrational peaks is comparable to or smaller than the instrument resolution of 18–28 meV (Ref. 13)]; overall, the spectrum exhibits a single vibrational progression with an average spacing of 1398 cm^{-1}. Similar observations, where two or more modes conspire to give the appearance of a single vibrational progression in incompletely resolved spectra, have been documented for a long time in luminescence spectra[39–41] and very recently in the intervalence absorption spectra of delocalized organic mixed-valence systems.[42] Since the mode that appears in the spectrum is (usually) not an actual mode of the system, this effect has been referred to as the missing mode effect (MIME).

IV. CONCLUSIONS

We have presented a theoretical study of the intermolecular reorganization energy for anthracene, tetracene and pentacene. The partitioning of the relaxation energy into normal mode contributions shows that the major contributions to λ_{rel} are due to several vibrational modes in the region 1200–1600 cm^{-1}. Our results reveal that the regular high-frequency vibrational progression observed in all three systems is a consequence of the collective action of several modes and resembles the missing mode effect.

The results of the vibrational analysis have been used to simulate the vibrational structure of the first ionization peak of the UPS spectra. The experimental and theoretical spectra are in good general agreement. Some remaining discrepancy could be due to nonadiabatic interactions, Duschinsky mixing, and anharmonic effects. Preliminary calculations of Duschinsky matrices (performed with the DUSHIN program developed by Reimers[19]), point to the presence of some mixing among the vibrations in the 1200–1600 cm^{-1} region (Tables VI–VIII). These results suggest that a simulation based on multidimensional Franck–Condon factors, computed taking into account the Duschinsky mixing, might further improve the agreement between theoretical and experimental spectra. Such investigations are currently in progress and will be reported elsewhere .

ACKNOWLEDGMENTS

The authors are most grateful to J. R. Reimers for kindly providing the DUSHIN program. This work has been partly supported by the National Science Foundation (through the STC and MRSEC programs under Awards No. DMR-0120967 and No. DMR-9809364, respectively, and through CHE-0078819), the Office of Naval Research, and the IBM Shared University Research program.

[1] W. P. Su, J. R. Schrieffer, and A. J. Heeger, Phys. Rev. Lett. **42**, 1698 (1979).
[2] J. L. Bredas and G. B. Street, Acc. Chem. Res. **18**, 309 (1985).
[3] W. R. Salaneck, R. H. Friend, and J. L. Bredas, Phys. Rep. **319**, 231 (1999).
[4] R. A. Marcus, Discuss. Faraday Soc. **29**, 21 (1960).
[5] R. A. Marcus and N. Sutin, Comments Inorg. Chem. **5**, 119 (1986).
[6] N. S. Hush, Coord. Chem. Rev. **64**, 135 (1985).
[7] P. F. Barbara, T. J. Meyer, and M. A. Ratner, J. Phys. Chem. **100**, 13148 (1996).
[8] E. A. Silinsh, A. Klimkans, S. Larsson, and V. Capek, Chem. Phys. **198**, 311 (1995).
[9] M. Pope and C. E. Swenberg, *Electronic Processes in Organic Crystals and Polymers*, 2nd ed. (Oxford University Press, New York, 1999).
[10] A. Devos and M. Lannoo, Phys. Rev. B **58**, 8236 (1998).
[11] T. Kato and T. J. Yamabe, J. Chem. Phys. **115**, 8592 (2001).
[12] V. Coropceanu, J. M. Andre, M. Malagoli, and J. L. Bredas, Theor. Chem. Acc. **110**, 59 (2003).
[13] V. Coropceanu, M. Malagoli, D. A. da Silva Filho, N. E. Gruhn, T. G. Bill, and J. L. Brédas, Phys. Rev. Lett. **89**, 275503 (2002).
[14] N. E. Gruhn, D. A. da Silva Filho, T. G. Bill, M. Malagoli, V. Coropceanu, A. Kahn, and J. L. Brédas, J. Am. Chem. Soc. **124**, 7918 (2002).
[15] S. F. Nelson, Y. Y. Lin, D. J. Gundlach, and T. N. Jackson, Appl. Phys. Lett. **72**, 1854 (1998).
[16] Y. C. Cheng, R. J. Silbey, D. A. da Silva Filho, J. P. Calbert, J. Cornil, and J. L. Brédas, J. Chem. Phys. **118**, 3764 (2003).
[17] L. Giuggioli, J. D. Andersen, and V. M. Kenkre, Phys. Rev. B **67**, 045110 (2003).
[18] M. Malagoli and J. L. Brédas, Chem. Phys. Lett. **327**, 13 (2000).
[19] J. R. Reimers, J. Chem. Phys. **115**, 9103 (2001).
[20] E. B. Wilson, J. C. Decius, and P. C. Cross, *Molecular Vibrations* (Dover, New York, 1980).
[21] F. Duschinsky, Acta Physicochim. URSS **7**, 551 (1937).
[22] A. D. Becke, Phys. Rev. A **38**, 3098 (1988).
[23] A. D. Becke, J. Chem. Phys. **98**, 1372 (1993).

[24] C. Lee, W. Yang, and R. G. Parr, Phys. Rev. B **37**, 785 (1988).
[25] R. Ditchfield, W. J. Hehre, and J. A. Pople, J. Chem. Phys. **54**, 724 (1971).
[26] W. J. Hehre, R. Ditchfield, and J. A. Pople, J. Chem. Phys. **56**, 2257 (1972).
[27] P. C. Harihara and J. A. Pople, Mol. Phys. **27**, 209 (1974).
[28] M. S. Gordon, Chem. Phys. Lett. **76**, 163 (1980).
[29] P. C. Hariharam and J. A. Pople, Theor. Chim. Acta **28**, 213 (1973).
[30] M. J. Frisch, G. W. Trucks, H. B. Schlegel *et al.*, GAUSSIAN 98, Revision A7 Gaussian Inc., Pittsburgh, PA, 1998.
[31] P. Chen, *Unimolecular and Bimolecular Ion–Molecule Reaction Dynamics* (Wiley, New York, 1994).
[32] D. K. W. Mok, E. P. F. Lee, F. T. Chau, D. C. Wang, and J. M. Dyke, J. Chem. Phys. **113**, 5791 (2000).
[33] G. M. Sando and K. G. Spears, J. Phys. Chem. A **105**, 5326 (2001).
[34] H. Kupka and P. H. Cribb, J. Chem. Phys. **85**, 1303 (1986).
[35] S. Schumm, M. Gerhards, and K. Kleinermanns, J. Phys. Chem. A **104**, 10648 (2000).
[36] C. J. Ballhausen, *Molecular Electronic Structures of Transition Metal Complexes* (McGraw-Hill, New York, 1979).
[37] A. Klimkans and S. Larsson, Chem. Phys. **189**, 25 (1994).
[38] M. W. Wong, Chem. Phys. Lett. **256**, 391 (1996).
[39] L. W. Tutt, D. Tannor, E. J. Heller, and J. I. Zink, Inorg. Chem. **21**, 3858 (1982).
[40] L. W. Tutt, J. I. Zink, and E. J. Heller, Inorg. Chem. **26**, 2158 (1987).
[41] L. Tutt, D. Tannor, J. Schindler, E. J. Heller, and J. I. Zink, J. Phys. Chem. **87**, 3017 (1983).
[42] S. E. Bailey, J. I. Zink, and S. F. Nelsen, J. Am. Chem. Soc. **125**, 5939 (2003).